Polarization jet events and excitation of weak SAR arcs

S. Sazykin,[1,2] B. G. Fejer,[1] Yu. I. Galperin,[3] L. V. Zinin,[4] S. A. Grigoriev,[4]
and M. Mendillo[5]

Received 13 November 2001; revised 24 January 2002; accepted 5 February 2002; published 27 June 2002.

[1] Polarization Jet (PJ), also known as Sub-Auroral Ion Drift (SAID), events are supersonic westward plasma drifts on the equatorward edge of the diffuse aurora in the evening and nighttime sector. Their optical F-region signatures are weak 630.0 nm red arcs colocated with regions of fast convection. These weak arcs resemble Stable Auroral Red (SAR) arcs observed during the recovery phase of magnetic storms, but have lower intensities, shorter lifetimes, and occur without a significant heat flux from the magnetosphere. Previous model studies underestimated the brightness of weak SAR arcs. We present calculations showing that ion-neutral collisional heating and ion composition changes during PJ events may be an additional source of 630.0 nm emission, and propose experimental tests that could verify our modeling results. *INDEX TERMS:* 2447 Ionosphere: Modeling and forecasting; 0310 Atmospheric Composition and Structure: Airglow and aurora; 2431 Ionosphere: Ionosphere/magnetosphere interactions (2736); 2443 Ionosphere: Midlatitude ionosphere; 2411 Ionosphere: Electric fields (2712)

1. Introduction

[2] The ionosphere at subauroral and middle latitudes exhibits a number of highly dynamic processes related to the convection electric field and the coupling of energetic (trapped) particles and thermal plasma. In contrast to highly time varying features, the term SAR (Stable Auroral Red) arcs has come to denote large and long-lasting 630.0 nm optical structures in the midlatitude and subauroral ionosphere [e.g., *Rees and Roble*, 1975; *Kozyra et al.*, 1997]. SAR arcs are subvisual, steady, longitudinally extended structures embedded in the main ionospheric trough at or near the plasmapause projection, in the recovery phase of magnetic storms. They can last for several consecutive days, with surface brightness of typically between a few hundred R and a few kR but up to 20 kR during great magnetic storms. Large electron temperature enhancements that accompany SAR arcs are thought to be the primary cause of the optical emission (through electron impact). The energy needed to excite these strong, long-lasting SAR arcs is extracted from the ring current via the interaction of high energy ring current ions with the cold plasma during storm recovery, although the exact transfer mechanisms are still unclear [*Kozyra et al.*, 1997].

[3] Simultaneous 630.0 nm all-sky and incoherent scatter observations from the Millstone Hill Observatory [42.6°N, 288.5°E, 56° invariant latitude] have shown the occurrence of faint (up to a few hundred Rayleighs) SAR arcs aligned with deep, narrow plasma troughs, elevated electron and ion temperatures, and significantly enhanced westward convection on the equatorward edge of the diffuse aurora [*Mendillo et al.*, 1987]. *Foster et al.* [1994] pointed out that these observations indicate a close association of these weak SAR arcs with Polarization Jets (PJ) [e.g., *Galperin et al.*, 1973, 1974, 1997], which are also called Sub-Auroral Ion Drift (SAID) events [*Spiro et al.*, 1979; *Anderson et al.*, 1991], and fossil (convection related) plasma density troughs. Similar SAR arc observations with simultaneous ionospheric vertical and oblique sounding and, when available, with nearby satellite ion drift measurements in Yakutsk (L = 3.0, MLT = UT + 9 h), Russia were reported by *Khalipov et al.* [2001]. They determined from satellite data that PJ events may occur with minimal (5–15 min) delay in relation to a substorm onset as defined by the AE index. On the other hand, *Anderson et al.* [1993] found this delay to be > 30 min. Physical mechanisms for the generation of PJ events were proposed by *Southwood and Wolf* [1978], *Deminov and Shubin* [1987], *Anderson et al.* [1993], and *De Keyser et al.* [1998], although conclusive theoretical analysis is still lacking.

[4] Model calculations of the intensities of weak arcs [e.g., *Mendillo et al.*, 1987; *Foster et al.*, 1994] using the standard formulation of SAR arcs of *Rees and Roble* [1975] failed to yield the observed emission levels. These studies suggested that an additional photon-generation mechanism may account for a substantial portion of the 630.0 nm emission seen in weak arcs. The origin of this additional source was not identified, with only ion precipitation induced emission suggested as a possible candidate.

2. Sources of 630.0 nm Airglow

[5] The source of the 630.0 nm airglow is excitation of O(^{1}D) atoms, which in the nighttime subauroral ionosphere are excited in dissociative recombination of O_2^+ and NO^+ ions and in collisions of atomic oxygen with thermal electrons. The altitude-dependent volume emission rate $\eta(z)$ is a sum of three terms:

$$\eta(z) = \eta_{O2}(z) + \eta_{NO}(z) + \eta_e(z). \tag{1}$$

$\eta(z)$ profiles will be computed by assuming photochemical equilibrium and equating production and loss of O(^{1}D).

[6] Recombination of O_2^+ is the primary source of nightglow in the subauroral thermosphere. In the F-region at night, O_2^+ ions are created in the charge-exchange reaction

$$O^+ + O_2 \rightarrow O_2^+ + O, \tag{2}$$

and their dissociative recombination with electrons of density N_e at the rate R_1 results in, on the average, α = 1.2 O(^{1}D) atoms (α is the quantum yield of O(^{1}D)). The channels of loss of O(^{1}D) include radiative relaxation O(^{1}D)$\rightarrow$O(^{3}P) and quenching by N_2, O_2, and electrons (rates Q^1_{N2}, Q^1_{O2}, and Q^1_E, respectively). Quenching by O

[1]Center for Atmospheric and Space Sciences, Utah State University, Logan, USA.
[2]Now at Physics and Astronomy Department, Rice University, Houston, Texas, USA.
[3]Space Research Institute, Russian Academy of Sciences, Moscow, Russia.
[4]Kaliningrad State University, Russia.
[5]Center for Space Physics, Boston University, Boston, Massachusetts, USA.

0094-8276/02/2001GL014388$05.00

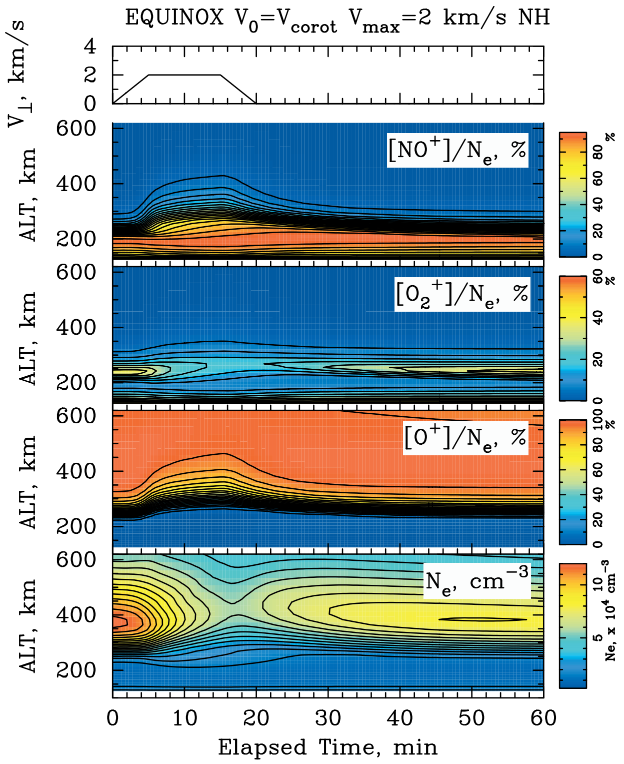

Figure 1. Changes in the electron and relative ion densities in response to imposed strong westward drift.

atoms is neglected following *Link and Cogger* [1988]. The emission rate η_{O2} (in photons/cm3/s) is then given by:

$$\eta_{O2} = \frac{\alpha R_1(T_e)[O_2^+]N_e A_{6300}}{A_{O1D} + Q_{N2}^1[N_2] + Q_{O2}^1[O_2] + Q_E^1 N_e}, \quad (3)$$

where A_{6300} and A_{O1D} are the Einstein probabilities for the $O(^3P \rightarrow {}^1D)$ and $O(^3P_2 \rightarrow {}^1D)$ radiative transitions, and $[O_2]$ and $[N_2]$ denote neutral densities.

[7] The contribution from NO^+ recombination is small under normal midlatitude nighttime conditions [*Solomon et al.*, 1988]. Most of the published calculations are either for dayglow conditions [e.g., *Frederick and Rusch*, 1977] or for the electron aurora [e.g., *Rees and Roble*, 1986]. Here, we calculate the possible contribution of NO^+ specifically for the nighttime subauroral conditions in the presence of PJ, where enhanced densities of molecular ions become important [e.g., *Anderson et al.*, 1991]. NO^+ ions are created in the charge exchange reaction

$$O^+ + N_2 \rightarrow NO^+ + N. \quad (4)$$

Excitation of $O(^1D)$ from recombination of NO^+ is a two-stage process. Dissociative recombination of NO^+ (at rate R_2) results in $N(^2D)$ excited atoms:

$$NO^+ + e^- \rightarrow \beta N(^2D) + (1-\beta)N + O(^3P) \quad (5)$$

(quantum yield $\beta \approx 0.76$). $N(^2D)$ is lost through radiation (transition probability A_{5200}) and quenching by N_2 (rate Q_{N2}^2), O_2 (rate Q_{O2}^2), O (rate Q_O^2), and electrons (rate Q_E^2). Equilibrium yields $[N(^2D)]$:

$$[N(^2D)] = \frac{\beta R_2(T_e)[NO^+]N_e}{A_{5200} + Q_{N2}^2[N_2] + Q_{O2}^2[O_2] + Q_O^2[O] + Q_E^2 N_e} \quad (6)$$

Quenching of $N(^2D)$ by O and O_2 is the source of $O(^1D)$ [e.g., *Solomon et al.*, 1988; *Solomon and Abreu*, 1989]:

$$N(^2D) + O_2 \rightarrow N(^4S) + \gamma_{O2}O(^1D) + (1-\gamma_{O2})O$$

$$N(^2D) + O \rightarrow NO + \gamma_O O(^1D) + (1-\gamma_O)O \quad (7)$$

with estimated quantum yields $\gamma_{O2} = 0.76$ and $\gamma_O = 0.1$. The second term in (1) is:

$$\eta_{NO} = \frac{\left(\gamma_O Q_{N2}^2[O] + \gamma_{O2}Q_{O2}^2[O_2]\right)[N(^2D)]A_{6300}}{A_{O1D} + Q_{N2}^1[N_2] + Q_{O2}^1(O_2) + Q_E^1 N_e}. \quad (8)$$

[8] Thermal electrons with $E \geq 1.97$ eV excite $O(^1D)$ [*Rees and Roble*, 1975] at the rate R_{th} [*Mantas and Carlson*, 1991], giving rise to the third term in (1):

$$\eta_e = \frac{R_{th}(T_e)N_e(O)A_{6300}}{A_{O1D} + Q_{N2}^1[N_2] + Q_{O2}^1[O_2] + Q_E^1 N_e}. \quad (9)$$

[9] The rates of reactions (2) and (4) depend strongly on the ion temperatures and relative ion drift velocities [*Rodger et al.*, 1992]; both are large in the regions of PJ. *Hierl et al.* [1997] measured these rates also as a function of neutral (vibrational) temperature. As far as we are aware, this is the first time temperature-dependent rates of (2) and (4) are accounted for in computing optical 630.0 nm emissions.

[10] Calculation of (1) requires knowledge of time dependent vertical profiles of ion densities and temperatures in the region of fast convection on the equatorward boundary of the diffuse aurora. For these purposes, we use numerical modeling to evaluate the required plasma parameters. This gives us the most flexibility; while incoherent-scatter radar data can be obtained under the right circumstances [e.g., *Providakes et al.*, 1989], such measurements are far from routine.

3. Results and Discussion

[11] Numerical MHD [e.g., *Moffett et al.*, 1992] and kinetic [*Korosmezey et al.*, 1992] models have been used to study the time development of idealized PJ events. The multi-fluid MHD model used in this work was described by *Grigoriev et al.* [1999]. The model solves the time-dependent continuity, momentum, and energy balance equations for electrons and 7 ion species (O^+, H^+, He^+, O_2^+, NO^+, N^+, N_2^+) along a single magnetic tube of flux connecting conjugate hemispheres at base altitudes of 125 km. For this study, the flux tube is at $L = 3.2$. MSIS-90 is adopted as the neutral atmosphere for moderate solar flux ($F10.7 = 150 \times 10^{-22}$ W/m2/Hz) conditions. Initially, equilibrium profiles are obtained by running the model for several days of physical time with the drift velocity set to zero. A PJ event is modeled as an imposed westward drift turned on at MLT = 22. The velocity increases linearly from 0 to its maximum value linearly in 5 min, remains constant for 10 min, and then decreases linearly to zero over 5 min. The rise time of 5 min is a simplified way to represent a PJ in the ionosphere; it has no relationship to the onset time discussed by *Anderson et al.* [1993]. Calculations are continued for 5 hours of physical time after that. The jet is terminated after 20 min to prevent the flux tube from convecting westward into the sunlight. Here, we present one single case; more detailed results for different conditions will be presented elsewhere.

[12] Figures 1 and 2 show the time evolution of ion densities and temperatures, respectively, in the northern hemisphere for the

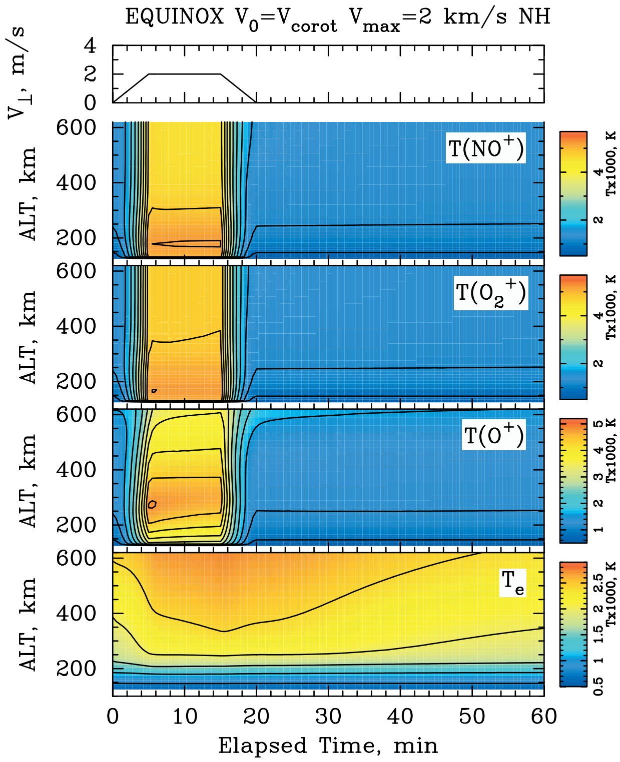

Figure 2. Ion temperatures during the modeled PJ.

case of equinox (day = 81), jet velocity of 2 km/s, and initial velocity set to corotation velocity. The main effects of the large meridional electric field are total electron density depletion, enhanced molecular ion concentrations in the F-region, and strong ion-neutral heating below the F-region peak. Radar-determined ion and electron temperature profiles, when available, are generally consistent with this picture of enhanced ion-neutral heating and transfer of energy to thermal electrons [*Providakes et al.*, 1989; *Foster et al.*, 1994], although, due to the experimental limitations, the radar-obtained temperatures are expected to be underestimated. The changes in the molecular ion composion are consistent with the results of *Anderson et al.* [1991].

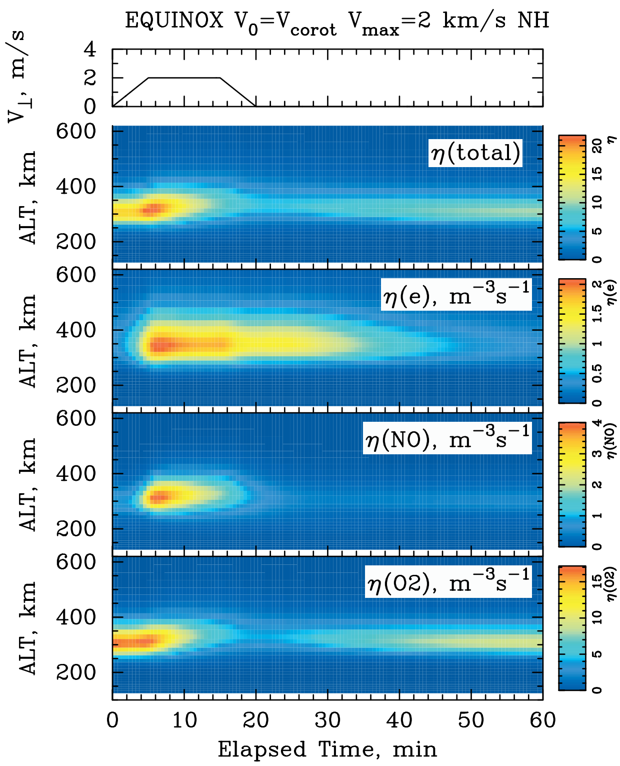

Figure 3. Contribution of the 3 mechanisms of excitation in (1) to the total emission profile.

[13] Figure 3 shows all 3 emission profiles in (1) computed separately. Figure 4 shows the time evolution of the total surface brightness obtained by integrating equation (1) over the range of altitude 125–800 km. Heating of the electron gas through the ion-neutral collisions results in a weak red line emission. However, enhanced recombination of molecular ions results in a decrease of the O_2^+ contribution but the contribution of NO^+ rises to the same level as that of the electron emission. The increase in the brightness is $\sim$80 R in the polarization jet. The brightness decreases afterwards to about 90 R. However, it should be kept in mind that the flux tube at this time will be displaced in MLT (by combined and opposing westward drift and corotation) into the post-midnight sector. The initial brightness level of 190 R is higher than that typically observed in this region due to our overestimation of the initial electron density. This is due to the fact that our numerical model is one-dimensional, whereas a two-dimensional picture of the ionospheric convection is required to account for the stagnation of flux tubes in the post-sunset subauroral ionosphere. Our more extensive calculations (not presented here) indicate that the physical picture of an enhanced 630.0-nm emission is valid even with a pre-existing electron density trough.

[14] These model calculations indicate that the ion-neutral frictional heating in the F-region may be capable of providing energy enough to excite weak emissions even without the heat flux from the magnetosphere postulated as the source of SAR arcs. Thus, PJ events may possibly be an additional source of weak red arcs observed in connection with fast ion drifts in the subauroral ionosphere (see [*Khalipov et al.*, 2001]). For weak SAR arcs, increased recombination of the NO^+ molecular ions may be as important as the thermal excitation mechanism. In contrast to the classical SAR arcs, PJ-associated arcs should be much weaker, shorter-lived, MLT-limited, and highly variable in response to changes in the convection velocity and plasma temperatures and densities. Furthermore, under realistic geophysical conditions, it is likely that both sources of energy of red arcs are at work since both PJ events and particle injection in the ring current are associated with periods of geomagnetic disturbances. On the other hand, *Providakes et al.* [1989] observed a PJ event but found no evidence of SAR arcs. Perhaps, our understanding of the conditions under which SAR arcs occur is not yet complete.

[15] As a test to distinguish PJ-related SAR arcs from ring current-induced arcs, we suggest that due to enhanced NO^+ recombination some enhancement of the highly forbidden 5200

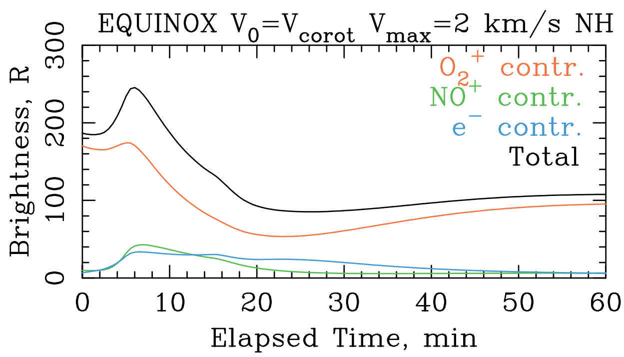

Figure 4. Surface brightness and its individual components (equation (1)) during the idealized PJ event.

NI spectral line is expected in PJ-related arcs due to optical relaxation of N(^{2}D). Another interesting point is that the Doppler profile of the 630.0 nm line can be significantly broadened in the PJ-related arcs in contrast to the classical ones. We propose to verify both ideas with spectrographic experiments. New observational techinques such as tomographic inversion should provide information on the 2-dimensional structure of SAR arcs [*Semeter et al.*, 1999], which can be directly compared with model results.

[16] **Acknowledgments.** This work was supported by JURRIS grant NAG5-8638 from NASA.

References

Anderson, P. C., R. A. Heelis, and W. B. Hanson, The ionospheric signatures of rapid subauroral ion drifts, *J. Geophys. Res.*, *96*, 5785–5792, 1991.

Anderson, P. C., W. B. Hanson, R. A. Heelis, J. D. Craven, D. N. Baker, and L. A. Frank, A proposed production model of rapid subauroral ion drifts and their relationship to substorm evolution, *J. Geophys. Res.*, *98*, 6069–6078, 1993.

De Keyser, J., M. Roth, and J. Lemair, The magnetospheric driver of subauroral ion drifts, *Geophys. Res. Lett.*, *25*, 1625–1628, 1998.

Deminov, M. G., and V. N. Shubin, Dynamics of the subauroral ionosphere under disturbed conditions, *Geomagnetism and Aeronomy*, *27*, 398, 1987.

Foster, J. C., M. J. Buonsanto, M. Mendillo, D. Nottingham, F. J. Rich, and W. Denig, Coordinated stable auroral red arc observations: Relationship to plasma convection, *J. Geophys. Res.*, *99*, 11,429–11,439, 1994.

Frederick, J. E., and D. W. Rusch, On the chemistry of metastable atomic nitrogen in the F region deduced from simultaneous satellite measurements of the 5200-A airglow and atmospheric composition, *J. Geophys. Res.*, *82*, 3509–3517, 1977.

Galperin, Yu. I., Y. N. Ponomarev, and A. G. Zosimova, Direct measurements of ion drift velocity in the upper atmosphere during a magnetic storm, *Cosmic Research*, *11*, 283–292, 1973.

Galperin, Yu. I., Y. N. Ponomarev, and A. G. Zosimova, Plasma convection in the polar ionosphere, *Ann. Geophys.*, *30*, 1–7, 1974.

Galperin, Yu. I., V. S. Soloviev, K. Torkar, J. C. Foster, and M. V. Veselov, Predicting the plasmaspheric density radial profiles, *J. Geophys. Res.*, *102*, 2079–2091, 1997.

Grigoriev, S. A., L. V. Zinin, I. Y. Vasilenko, and V. E. Lynovsky, Multi-ion one-dimensional MHD models of upper ionosphere dynamics: 1. A mathematical ionospheric model with seven positive ion species, *Cosmic Research*, *37*, 425, 1999.

Hierl, P. M., I. Dotan, J. V. Seeley, J. M. Van Doren, R. A. Morris, and A. A. Viggiano, Rate constants for the reactions of O^+ with N_2 and O_2 as a function of temperature (300–1800 K), *J. Chem. Phys.*, *106*, 3540–3544, 1997.

Khalipov, V. L., Yu. I. Galperin, A. E. Stepanov, and L. V. Shestakova, Formation of the Polarization Jet during substorm expansion phase: Results of ground-based measurements, *Cosmic Research*, *39*, 226–235, 2001.

Korosmezey, A., C. E. Rasmussen, T. I. Gombosi, and G. V. Khazanov, Anisotropic ion heating and parallel O^+ acceleration in regions of rapid $E \times B$ convection, *Geophys. Res. Lett.*, *19*, 2289–2292, 1992.

Kozyra, J. U., A. F. Nagy, and D. W. Slater, High-altitude energy source(s) for stable auroral red arcs, *Rev. Geophys.*, *35*, 155–190, 1997.

Link, R., and L. L. Cogger, A reexamination of the OI 6300 Å nightglow, *J. Geophys. Res.*, *93*, 9883–9892, 1988.

Mantas, G. P., and H. C. Carlson, Reexamination of the O(^{3}P→^{1}D) excitation rate by thermal electron impact, *Geophys. Res. Lett.*, *18*, 159–162, 1991.

Mendillo, M., J. J. Baumgardner, J. C. Aarons, J. C. Foster, and J. Klobuchar, Coordinated optical and radio studies of ionospheric disturbances: Initial results from Millstone Hill, *Ann. Geophys.*, *5A*, 543–550, 1987.

Moffett, R. J., R. A. Heelis, R. Sellek, and G. J. Bailey, The temporal evolution of the ionospheric signatures of subauroral ion drifts, *Planet. Space Sci.*, *40*, 663–670, 1992.

Providakes, J. F., M. C. Kelley, W. E. Swartz, M. Mendillo, and J. Holt, Radar and optical measurements of ionospheric processes associated with intense subauroral electric fields, *J. Geophys. Res.*, *94*, 5350–5366, 1989.

Rees, M. H., and R. G. Roble, Observations and theory of the formation of stable auroral red arcs, *Rev. Geophys.*, *13*, 201, 1975.

Rees, M. H., and R. G. Roble, Excitation of (O^{1}D) atoms in aurorae and emission of the [OI] 6300-Å line, *Can. J. Phys.*, *64*, 1608–1613, 1986.

Rodger, A. S., R. J. Moffett, and S. Quegan, The role of ion drift in the formation of ionization troughs in the mid- and high-latitude ionosphere — a review, *J. Atmos. Terr. Phys.*, *54*, 1–30, 1992.

Semeter, J., M. Mendillo, and J. Baumgardner, Multispectral tomographic imaging of the midlatitude aurora, *J. Geophys. Res.*, *104*, 24,565–24,585, 1999.

Solomon, S. C., and V. J. Abreu, The 630 nm dayglow, *J. Geophys. Res.*, *94*, 6817–6824, 1989.

Solomon, S. C., P. B. Hays, and V. J. Abreu, The auroral 6300 emission: Observations and modeling, *J. Geophys. Res.*, *93*, 9867–9882, 1988.

Southwood, D. J., and R. A. Wolf, An assessment of the role of precipitation in magnetospheric convection, *J. Geophys. Res.*, *83*, 5227, 1978.

Spiro, R. W., R. A. Heelis, and W. B. Hanson, Rapid subauroral ion drifts observed by Atmospheric Explorer C, *Geophys. Res. Lett.*, *6*, 657, 1979.

B. G. Fejer and S. Sazykin, Center for Atmospheric and Space Sciences, Utah State University, Logan, UT 84322-4405, USA. (bfejer@cc.usu.edu; sazykin@rice.edu)

M. Mendillo, Center for Space Sciences, Boston University, Boston, MA 02215, USA.

Yu. I. Galperin, Space Research Institute, Russian Academy of Sciences, Moscow, 117997, Russia.

S. A. Grigoriev and L. V. Zinin, Kaliningrad State University, Kaliningrad, 236041, Russia.